NJ.
Grant, G. A., & Chiappinelli, V. A. (1985) *Biochemistry 24*, 1532–1537.
Grant, G. A., Frazier, M. W., & Chiappinelli, V. A. (1988) *Biochemistry 27*, 3794–3798.
Inagaki, F., Hider, R. C., Hodges, S. J., & Drake, A. F. (1985) *J. Mol. Biol. 183*, 575–590.
Karlsson, E. (1979) *Handb. Exp. Pharmacol. 52*, 159–212.
Karlsson, E., Eaker, D., & Ponterius, G. (1972) *Biochem. Biophys. Acta 257*, 235–248.
Loring, R. H., Andrews, D., Lane, W., & Zigmond, R. E. (1986) *Brain Res. 385*, 30–37.
Love, R. A., & Stroud, R. M. (1986) *Protein Eng. 1*, 37–46.
Ravdin, P. M., & Berg, D. K. (1979) *Proc. Natl. Acad. Sci. U.S.A. 76*, 2072–2076.
Rees, B., Samama, J. P., Thierry, J. C., Gilibert, M., Fischer, J., Schweitz, H., Lazdunski, M., & Moras, D. (1987) *Proc. Natl. Acad. Sci. U.S.A. 84*, 3132–3136.
Wolf, K. M., Ciarleglio, A., & Chiappinelli, V. A. (1988) *Brain Res. 439*, 249–258.

Influence of Globin Structure on the Heme in Dromedary Carbonmonoxyhemoglobin[†]

G. Amiconi,*[‡,§] R. Santucci,[§] M. Coletta,[‡] A. Congiu Castellano,[∥] A. Giovannelli,[∥] M. Dell'Ariccia,[∥] S. Della Longa,[∥] M. Barteri,[⊥] E. Burattini,[#] and A. Bianconi[○]

Dipartimento di Scienze Biochimiche, Gruppo Nazionale di Cibernetica e Biofisica, Dipartimento di Fisica, and Dipartimento di Chimica, Università degli Studi La Sapienza, 00185 Roma, Italy, CNR, Centro di Biologia Molecolare, 00185 Roma, Italy, CNR-INFN, Laboratori Nazionali di Frascati, 00044 Frascati, Italy, and Dipartimento STBB, Facoltà di Medicina, 67100 L'Aquila, Italy

Received November 23, 1988; Revised Manuscript Received June 14, 1989

ABSTRACT: By use of X-ray absorption near-edge structure (XANES), circular dichroism, and visible absorption spectroscopies, dromedary carbonmonoxyhemoglobin has been characterized structurally and functionally. By consideration of the experimental results the following view emerges: (i) the quaternary structure is not the unique factor determining the tertiary environment around the heme, and (ii) the multiplicity of interactions between hemoglobin and solvent components induces a large number of globin conformations, which somehow affect the conformation of the heme such that the structural parameters (i.e., the doming of porphyrins, the movements of the iron relative to the heme plane, the distortion of the ligand field, and the change in the Fe–C–O angle) can be uncoupled.

Cooperativity in hemoglobin, i.e., the increase in binding energy of the fourth heme ligand relative to the first (Antonini & Brunori, 1971; Perutz et al., 1987), arises from a linkage between the stereochemistry at the heme and various protein conformations, which differ in the tertiary structure of the α and β subunits and in the quaternary structure of the tetramer (Ackers & Smith, 1987; Perutz et al., 1987). A large body of equilibrium and kinetic data supports the idea that hemoglobin exists in two main quaternary structures, T (tense) and R (relaxed) state(s), which are different for heme–ligand affinity and that cooperativity is associated with a switch from the T to the R state(s) at some point on the binding curve (Perutz, 1979; Brunori et al., 1985). X-ray diffraction studies have revealed that in the unligated derivative the porphyrins are domed and, regardless of the quaternary structure, the iron atoms are displaced by 0.04 nm from the plane of the porphyrin nitrogens toward the proximal histidines. On ligand binding, the irons move toward the porphyrin planes, which remain domed in the T structure but flatten on transition to the R structure (Perutz et al., 1987). Such perturbations at the hemes are coupled to a net movement of the FG corner together with a portion of the F helix (i.e., with tertiary conformational modifications), thus triggering changes in the quaternary structure (Baldwin & Chothia, 1979; Gelin et al., 1983; Arnone et al., 1986). Therefore, as hemes are successively bound to a ligand molecule, the interactions that stabilize the T quarternary structure are lost (due to the strain at the active site), relieving the protein constraints and consequently increasing the affinity for heme ligands. On the other hand, interactions between hemoglobin and solvent components may bring about tertiary and quaternary structural variations, which propagate to the hemes and to intersubunit interfaces modulating in this way the reactivity of hemoglobin for heme ligands. In general, each quaternary state (T or R) may differ in tertiary conformation of the subunits (t or r), depending on the lower or higher intrinsic heme–ligand affinity of the subunits, and therefore, the system may be described in terms of (at least) four alternative states [denoted as follows: Rr and Rt, for conformations at high and low affinity for heme ligands of the subunits within the R structure; Tt and Tr, for low- and high-affinity conformations of chains within the T structure (Perutz, 1972; Santucci et al., 1985, 1986a,b; San-

[†] This research was supported by grants from the Ministero della Pubblica Istruzione (40% and 60%).
[‡] Dipartimento di Scienze Biochimiche, Università degli Studi La Sapienza.
[§] CNR, Centro di Biologia Molecolare.
[∥] Gruppo Nazionale di Cibernetica e Biofisica, Dipartimento di Fisica, Università degli Studi La Sapienza.
[⊥] Dipartimento di Chimica, Università degli Studi La Sapienza.
[#] CNR-INFN, Laboratori Nazionali di Frascati.
[○] Dipartimento STBB, Facoltà di Medicina.

0006-2960/89/0428-8547$01.50/0 © 1989 American Chemical Society

tucci & Amiconi, 1988)]. However, the detailed mechanism of cooperativity remains a matter of debate as to whether intermediate structures (i.e., partially ligated states in hemoglobin) have major or minor influence on heme–heme interaction (Perutz et al., 1987; Gelin & Karplus, 1977; Rousseau & Ondrias, 1983; Warshel, 1977). In agreement with this view, a model has been proposed which suggests that destabilization of the ligated T structure, as observed in the partially ligated intermediate, is responsible for the low affinity of hemoglobin at the beginning of the ligation process; in other words, the most significant strain is to be sought not in the fully unligated but in the partially ligated T structure (Gelin & Karplus, 1977).

In order to shed more light on the cooperativity mechanism, more information on relationships between heme stereochemistry and the local protein environment of ligated, partially ligated, and unligated hemoglobin (in both the R and T quaternary structures) is required. Dromedary hemoglobin appears to be a good system for such a task, in view of its high degree of molecular flexibility, at least within the R quaternary structure (Santucci et al., 1985, 1986a,b; Santucci & Amiconi, 1988). This hemoglobin is an $\alpha_2\beta_2$ tetramer displaying all the amino acids (Braunitzer et al., 1979) considered relevant for the functional properties of human hemoglobin but being characterized by the presence of two distinct binding sites for polyanions, which modulate the structural and functional properties of the protein as a function of their concentration (Amiconi et al., 1985; Santucci et al., 1985; Desideri et al., 1987; Ascenzi et al., 1988).

In particular, previous results (Bertollini et al., 1988) on dromedary oxyhemoglobin [i.e., in R state(s)] indicate that (i) the effect of polyanions on the protein conformation appears to be essentially local (tertiary conformational changes, i.e., Rr $\rightleftharpoons$ Rt) and (ii) the presence of chloride ions is necessary in order to induce quaternary changes in the polyanion–protein system (i.e., R $\rightleftharpoons$ T).

In what follows X-ray absorption near-edge structure (XANES)[1] spectroscopic results on the carbonmonoxy derivative (HbCO) of dromedary hemoglobin are reported in the presence of different solvent components and compared with dichroic spectra in the near-UV region as well as with kinetic data obtained under the very same conditions. The measurement of circular dichroism spectra is of particular advantage as a tool to investigate the structural organization of hemoglobin so as to give detailed information on tertiary and quaternary structural changes (Geraci & Parkhurst, 1981). On the other hand, XANES spectroscopy is uniquely suited for probing structural changes around the iron atom with precision higher than that provided from conventional X-ray diffraction on single crystals. Next, the carbon monoxide dissociation rate is a necessary complement to these structural studies in that the rate-limiting step in ligand dissociation reactions is most likely the breaking of the metal–ligand bond; dissociation rates, therefore, provide more intimate and direct information concerning the steric and electronic environment of the heme pocket. The HbCO form has been chosen because of (i) its stability, (ii) the absence of iron oxidation during the experiments (due to the presence of dithionite in the system), and (iii) its stereochemistry on the distal side of the heme, which should give rise to strong interactions between CO and His E7 (distal histidine) or Val E11.

[1] Abbreviations: XANES, X-ray absorption near-edge structure; HbCO, carbonmonoxyhemoglobin; IHP, inositol hexakisphosphate sodium salt; Bis-Tris, 2,2-bis(hydroxymethyl)-2,2′,2″-nitrilotriethanol; CFA, chlofibric acid [2-(*p*-chlorophenoxy)-2-methylpropionic acid]; EXAFS, extended X-ray absorption fine structure.

Materials and Methods

Specimens of dromedary blood were collected from the jugulary veins of animals in acid/citrate/dextrose.

Hemoglobin was purified as previously described (Antonini & Brunori, 1971) and then stripped from any ion bound to the protein by passing the solution through a column of mixed-bed ion-exchange resin (Bio-Rad AG501 X8) (Amiconi & Giardina, 1981).

Protein concentration was estimated spectrophotometrically by using an extinction coefficient of 13.4 mM^{-1} cm^{-1} at 569 nm for the carbonmonoxy derivative. Inositol hexakisphosphate and chlofibric acid were purchased from Sigma Chemical Co. (St. Louis, MO). The other reagents were from Merck AG (Darmstadt, FRG). All chemicals were of analytical grade and were used without further purification.

A Cary 219 spectrophotometer (Varian) was used for all optical measurements.

The XANES experiments were performed at the Frascati synchrotron radiation facility using the Wiggler beam line. The synchrotron radiation was monochromatized by a Si (111) channel-cut single crystal. The high stability of the electron beam in the storage ring has provided a high signal-to-noise ratio and a good reproducibility of the absorption spectra collected in transmission. The zero of the energy scale was carefully fixed at the threshold of the Fe metal K edge defined as the first maximum of its derivative spectrum. The absorption background due to lower binding energy levels has been subtracted by polynomial fitting of the preedge region. The absorption coefficient in the spectra was normalized to α_0, defined as the atomic absorption jump obtained by linear fitting of EXAFS oscillation in the range 50–150 eV. This accurate normalization procedure provides unambiguous variations of the intensities of XANES peaks to be detected. The energy resolution was about 1 eV, and energy shifts of absorption spectral features as low as 0.2 eV could be detected. A good signal-to-noise ratio ($\Delta\alpha = \pm 0.005\Delta\alpha_0$) was obtained by reaching very good stability of the electron beam in the storage ring and in the Wiggler magnetic field.

Circular dichroism spectra were recorded with a Jasco J-500 A spectropolarimeter equipped with a Jasco DP-500 N processor. The molar ellipticity (deg·cm^2·$dmol^{-1}$) is expressed as $(\theta)_h$ on a molar basis.

CO dissociation kinetics was carried out at 20 °C and pH 6.5 with two different methods, namely, (i) CO displacement by deoxy microperoxidase by virtue of its higher affinity for CO (Sharma et al., 1975), following the formation of CO microperoxidase at $\lambda = 550$ nm, and (ii) CO displacement by hexaferricyanide (Antonini & Brunori, 1971), detecting the formation of aquomet Hb at $\lambda = 569$ nm. The two methods gave overlapping results, confirming that in both cases the observed kinetics was limited by the same process, that is, the CO dissociation.

Results

Circular Dichroism Measurements. Circular dichroism spectra of dromedary HbCO were carried out in the near-UV region (250–300 nm) in the absence and in the presence of various allosteric effectors as shown in Figure 1. Even though it is generally acknowledged that the interpretation of changes in dichroic spectra in proteins may be quite complicated, in this case the set of structural monitors used appears to be well documented. Thus, changes in the 280–300-nm region are related to variations in the environment of Trp β37(C3) located at the $\alpha_1\beta_2$ contact surface and therefore involved in the

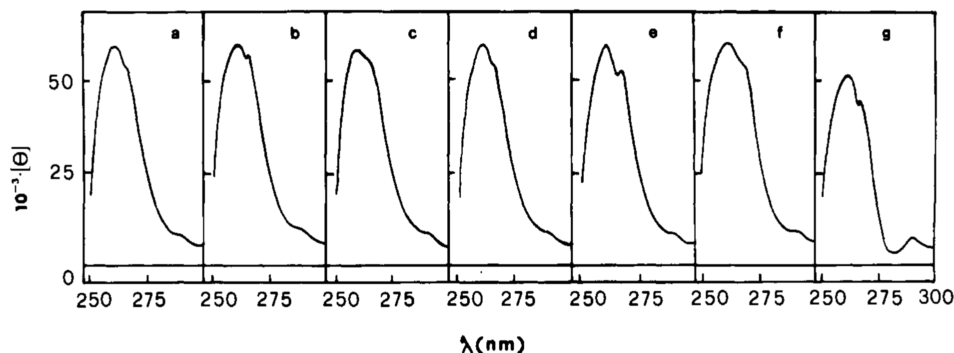

FIGURE 1: Effect of solvent components on the near-UV circular dichroic spectra of dromedary HbCO (0.2 mM in heme) at pH 6.5 and 20 °C. The composition of the various solvents was as follows: (a) 0.01 M Bis-Tris buffer, pH 6.5; (b) buffer + 0.2 mM IHP; (c) buffer + 1 mM IHP; (d) buffer + 1 mM IHP + 100 mM chloride; (e) buffer + 15 mM CFA; (f) buffer + 15 mM CFA + 1 mM IHP; (g) buffer + 18 mM CFA + 1 mM IHP + 100 mM chloride.

quaternary transitions (Perutz et al., 1974), while changes in bands between 250 and 270 nm are mainly linked to tertiary modifications (Santucci et al., 1985; Geraci & Parkhurst, 1981).

The influence of a single anion or two allosteric effectors (see Figure 1) on the protein conformation appears to be limited to local tertiary changes, since dichroic variations (in shape and/or intensity) are observed only in the 250–270-nm range. In the absence of allosteric effectors, the dromedary HbCO shows a positive maximum at 260 nm and a shoulder at approximately 264 nm (Figure 1a). Upon addition of a stoichiometric amount of polyphosphate, the ellipticity at 264 nm increases and becomes a distinct peak (Figure 1b), which has been shown (Santucci et al., 1985) to be typical of the deoxy derivative; upon further addition of IHP, the peak at 264 nm disappears and the dichroic band assumes again the shape of a shoulder as already observed in the absence of allosteric effectors (Figure 1c). Therefore, it is evident that in the presence of a molar excess of IHP the tertiary conformation of dromedary HbCO becomes reminiscent of that typical of high-affinity structure. If 0.1 M chloride is added to the last system (Figure 1d), the dichroic spectrum becomes pratically undistinguishable from that typical of the protein in buffer only. Thus, quite interestingly, the modification of the dichroic spectrum in this region appears to be reversible as a function of IHP concentration, and therefore the protein may assume different (high affinity, Rr, or low affinity, Rt) local conformations. Under these conditions, no changes are observable in the 280–300-nm region, indicating that the quaternary R structure of the protein indeed is maintained.

Similarly to IHP, CFA [an antihyperlipoproteinemia drug in current use that favors a right-shifting effect on the oxygen equilibrium curve of human (Abraham et al., 1983; Perutz & Poyart, 1983) and dromedary (Bertollini et al., 1988) hemoglobin] affects the conformation of dromedary hemoglobin mainly at a tertiary level (see Figure 1e), but the changes induced by this effector toward a deoxy tertiary structure (Rt) appear to be more drastic as indicated by the steep minimum observed in the dichroic spectrum at approximately 262 nm (see also Figure 2). The simultaneous presence of IHP and CFA, in the absence and in the presence of chloride ions, brings about alterations of circular dichroic spectra, as shown in Figures 1f and 1g. It is important to notice that in the presence of all three effectors the changes on the dichroic spectrum of the protein are observable over the whole range investigated (250–300 nm) (Figure 1g). In particular, the decreasing in intensity of the band at approximately 287 nm [associated with Trp β37(C3) located at the $\alpha_1\beta_2$ interface (Perutz et al., 1974; Santucci et al., 1985)]

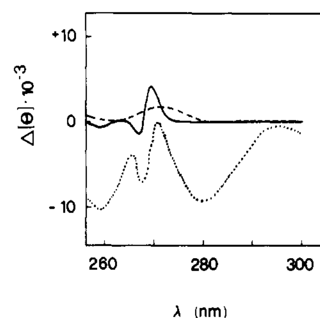

FIGURE 2: Differential dichroic spectra of dromedary HbCO (0.2 mM in heme) in various solvents relative to the protein in 0.01 M Bis-Tris buffer, pH 6.5: (dashed line) buffer + 1 mM IHP + 15 mM CFA; (continuous line) buffer + 15 mM CFA; (dotted line) buffer + 1 mM IHP + 15 mM CFA + 100 mM chloride.

clearly reveals a quaternary change in the tetramer, pushed toward the T-state quaternary structure. On the other hand, in the absence of chloride, IHP and CFA stabilize a tertiary oxy conformation, Rr, as revealed by a dichroic spectrum (Figure 1f) strongly reminiscent of that observed in the absence of any allosteric effector (Figure 1a).

In summary, IHP at low concentration or CFA alone stabilizes an intrasubunit structure typical of low affinity for ligands, Rt. Moreover, addition of both IHP and chloride to solvent containing CFA magnifies the dichroic features typical of the Rt structure and induces a partial switch toward the T quaternary structure, whereas the simultaneous presence of only CFA and IHP (i.e., without chloride) into the solvent pushes back the protein conformation toward an Rr structure and does not affect at all the R $\rightleftharpoons$ T transition. This evidence is made clearer by the differential dichroic spectra reported in Figure 2.

XANES Measurements. In Figures 3 and 4 are reported the absorption XANES spectra (and their derivatives) for dromedary HbCO in the absence and in the presence of one or more different anions (IHP, CFA, IHP + CFA, IHP + CFA + chloride).

Attention has been focused on three regions of the experimental XANES spectra: (i) the energy region of peak A on the absorption rising edge at about 10 eV (1 eV = 1.602 × 10^{-19} J), (ii) the region of peaks C_1 and D at 16 and 22 eV, respectively, and (iii) the region of peak P at $-0.3 < E < 3$ eV. The basic assumption underlying any local structure determination by XANES spectroscopy is that the same structure in different systems will give the same XANES spectrum, even if long-range order and the electronic properties of the systems are different. By using model compounds that have the same type of neighboring atoms in different geo-

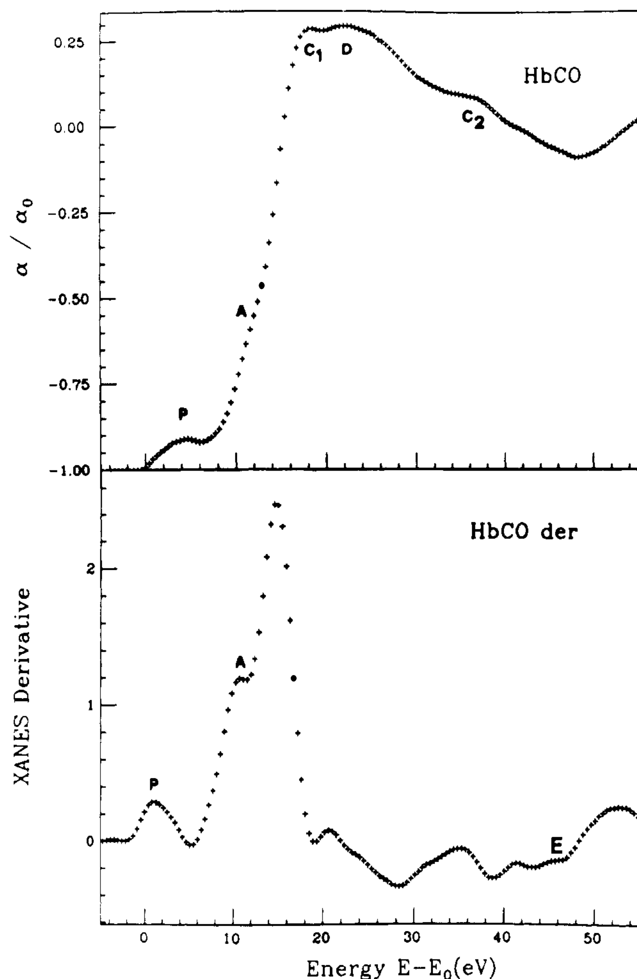

FIGURE 3: Fe K-edge XANES spectrum (upper panel) of dromedary HbCO (10 mM in heme) in 0.01 M Bis-Tris, pH 6.5, and its derivative (lower panel). The main experimental features are indicated by capital letters (see also text).

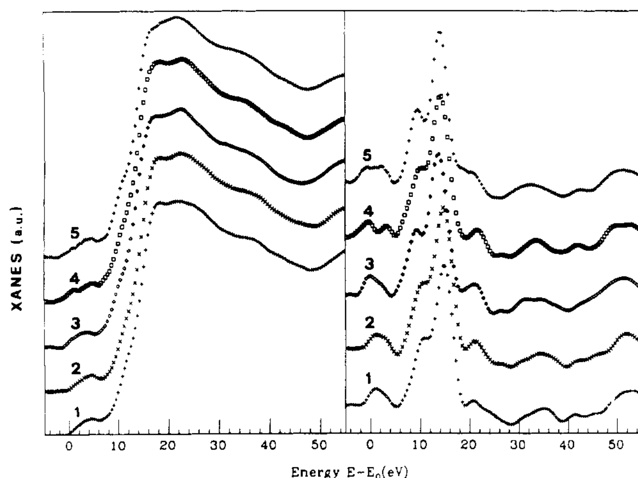

FIGURE 4: Experimental XANES spectra (left panel) and their derivatives (right panel) of dromedary HbCO (10 mM in heme) under different solvent conditions: (1) 0.01 M Bis-Tris buffer, pH 6.5; (2) buffer + IHP (equimolar with tetrameric hemoglobin); (3) buffer + 75 mM CFA; (4) buffer + IHP (in large molar excess relative to tetrameric protein) + 75 mM CFA; (5) buffer + IHP (in larger molar excess relative to tetrameric protein) + 75 mM CFA + 200 mM chloride.

metrical arrangements, it has been possible to demonstrate that XANES spectra are sensitive to changes in the interatomic distances, bonding angles, and subtle atomic displacements [see Bianconi (1987) and references quoted therein]. The

Table I: Values of the Intensity Ratio D/α_0 (Related to the Heme Doming) As Obtained from XANES Spectra for Dromedary HbCO (10 mM Bis-Tris/HCl, pH 6.5) in the Presence of Various Allosteric Effectors

solvent composition	D/α_0
buffer + CFA	1.513
buffer + IHP (in molar excess) + CFA + Cl^-	1.467
buffer + IHP (equimolar with tetrameric HbCO)	1.399
buffer + IHP (in molar excess) + CFA	1.367
buffer	1.337

Table II: Effect of Solvent Components on Fe–C–O Bonding Angle and Values of the Intensity Ratio C_1/α_0 (Used To Calculate the Structural Parameter) in Dromedary HbCO (10 mM Bis-Tris/HCl, pH 6.5)

solvent composition	C_1/α_0	bonding angle (deg)
buffer	1.297	159.2 ± 0.6
buffer + IHP (equimolar with tetrameric HbCO)	1.293	158.3 ± 0.6
buffer + IHP (in molar excess) + CFA	1.300	159.9 ± 0.6
buffer + CFA	1.259	153.5 ± 0.5
buffer + IHP (in molar excess) + CFA + Cl^-	1.257	153.0 ± 0.5

features of the theoretical XANES spectra are determined by the relative positions of the atoms in a cluster of about 30 atoms. In the case of HbCO this cluster is constituted by the atoms of the porphyrin plane, the proximal histidine, the iron ion, and the diatomic molecule CO. As elsewhere reported (Bianconi et al., 1985a,b, 1987), the theoretical spectra reproduce the experimental features labeled A, C_1, C_2, D, E, and P (see Figure 3) due to the multiple scattering of the photoelectron at the absorbing atom modulated along the direction normal to the heme plane and in the heme plane by neighboring atoms. In particular, (i) feature A, which appears as an inflection point in the first derivative of the spectrum (see Figure 3), is due to the scattering of the photoelectron in the direction normal to the porphyrin plane; the theoretical polarized spectrum shows that this feature gradually disappears with increase of the Fe–N_ϵ distance, in parallel with a shift of the absorption edge toward lower energy values (Bianconi et al., 1985d; Morante et al., 1987); (ii) peaks C_1 and C_2 are attributed to multiple scattering resonances in the direction normal to the heme plane and therefore are a good probe of the Fe–C–O bonding angle (Bianconi et al., 1985c); (iii) peak D, due to multiple scattering in the heme plane, is sensitive to doming of the porphyrin plane, and its intensity increases with the macrocycle distortion (Cartier et al., 1988). In addition, the preedge peak P (quadrupole-allowed transitions from Fe 1s to empty 3d states) is related to the distortion of the octahedral ligand field (Oyanagi et al., 1987).

The comparison (see Figure 4) between XANES spectra of HbCO and HbCO + IHP (the IHP being in equimolar concentration with the tetrameric protein) shows some difference at the level of peaks C_1 and D, indicating structural alteration in the neighborhood of the iron center, mainly referable to a smaller Fe–C–O bonding angle and some doming of the heme plane in the case of IHP in the solvent (see Tables I and II). On the other hand, addition of CFA to HbCO induces spectral changes (Figure 4) mostly for features A, C_1, and D. In particular, feature A is sharper than that present in both HbCO and HbCO + IHP, while peaks C_1 and D show higher intensity. In other words, CFA appears to affect the system (i) by doming to the highest degree the porphyrin plane (see Table I) and (ii) by favoring a movement of the iron from the heme plane (see Table III). On the other hand, the copresence of both IHP and CFA indicates an evident modification of band P, which appears split into two peaks (P_1 and

Table III: Contraction (Relative to the Protein in Pure Buffer) of the Fe–N_ϵ Distance and Energy Shift (Experimentally Measured Quantity) in Dromedary HbCO (10 mM Bis-Tris/HCl, pH 6.5) Induced by Allosteric Effectors

solvent composition	contraction values of Fe–N_ϵ (Å)	energy shift[a] (eV)
buffer + IHP (equimolar with tetrameric protein)	0.01[b]	≤0.2
buffer + IHP (in molar excess) + CFA	0.013 ± 0.001	0.23
buffer + CFA	0.018 ± 0.001	0.32
buffer + IHP (in molar excess) + CFA + Cl^-	0.036 ± 0.002	0.65

[a] According to theoretical calculation of XANES, a multiple scattering resonance at energy E_r moves to higher energy with decreasing interatomic distance d following the rule $E_r - E_b$ = a constant, where E_b is the energy of a localized excitation at threshold. A contraction of 0.1 Å of the average Fe–N_ϵ distance in a cluster of the atoms gives a shift of 1.8 eV of the rising absorption edge (Bianconi et al., 1985d). [b] This value indicates the upper limit for the Fe–N_ϵ distance variation, since the energy shift of the absorption jump measured (i.e., 0.2 eV) corresponds to the limit of sensitivity.

P_2), while features A and C_1 are similar to those found in HbCO. According to theory (Bianconi et al., 1985c; Cartier et al., 1988), the only allowed dipolar transitions toward molecular orbitals of d symmetry are z polarized if the z^2 symmetry MO is the final state and x, y polarized if the xz, yz symmetry MO's are the final state. Therefore, the first z-polarized transition (P_1) may be assigned to a transition toward the z^2 MO, and peak P_2 may be attributed to a transition toward degenerate MO's of xz, yz symmetry, combining the MO from carbon monoxide and xz and yz orbitals from iron. The clear-cut splitting of the preedge transition into two peaks (see Figure 4) is a remarkable feature, since it is not observed under the other solvent conditions used (where only one transition is detectable in this energy range). In conclusion, the addition of a molar excess of IHP to HbCO + CFA induces (i) a twist of the octahedral ligand field that has been seen favored by the aromatic anion (see Figure 4) and (ii) a reduction of the heme doming stabilized by CFA (see Table I).

The strongest modification of the full XANES spectrum is observed in the presence of all three allosteric effectors, i.e., IHP, CFA, and chloride (Figure 4). Thus, band P is split into two peaks (P_1 and P_2) that are not resolved as those observed in the presence of only two allosteric effectors (i.e., IHP and CFA; see Figure 4); moreover, peak A shows the sharpest shape and feature C_1 the lowest intensity, relative to all solvents studied. Therefore, the XANES characteristics of dromedary hemoglobin, observed in the presence of IHP, CFA, and chloride, indicate that, under these conditions, the porphyrins are considerably domed (see Table I), iron is much displaced away from the heme plane (Table III), and the Fe–C–O bonding angle is much lower than that of the carbonmonoxy derivative in buffer only (see Table II).

Kinetic Experiments. Cooperativity in the heme–ligand dissociation rate of human HbCO is greatly reduced compared to HbO_2, the stepwise dissociation rate constants for the four ligand molecules being similar within a factor of 2.5 (Sharma et al., 1975). In other words, the overall CO dissociation rate constant l is the same as the statistically corrected value of l_4 for the release of the first CO molecule from fully saturated hemoglobin (Antonini & Gibson, 1960). In addition, l, which is the same in human HbCO as l_4, is not affected by 2,3-diphosphoglycerate (Sharma et al., 1976). For these reasons, the reported measurements have been confined to the overall CO dissociation rate constants.

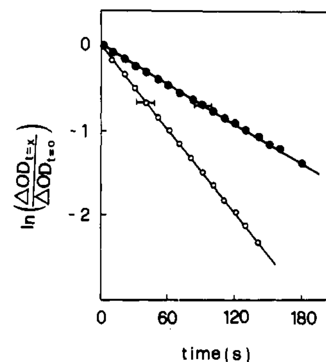

FIGURE 5: Time course of the dissociation of carbon monoxide from dromedary HbCO (0.2 mM in heme, in 0.01 M Bis-Tris buffer, pH 6.5), under two different solvent conditions [(●) buffer; (O) buffer + 10 mM CFA + 1 mM IHP + 100 mM Cl^-] at 20 °C.

Table IV: Kinetic Parameters for CO Dissociation from Dromedary HbCO (20 μM in 10 mM Bis-Tris/HCl, pH 6.5 and 20 °C) under Different Solvent Conditions

solvent conditions	$t_{1/2}$ (s)	$l \times 10^3$ (s^{-1})	ΔG^* (kJ·mol^{-1})
buffer	80	8.7 ± 1.0	11.5
+100 mM Cl^-	90	7.8 ± 1.0	11.5
+40 mM IHP	62	11 ± 1.0	10.9
+1 mM IHP	140	5 ± 1.0	13.2
+10 mM CFA	43	16 ± 2.0	10.0
+10 mM CFA + 1 mM IHP	85	8.1 ± 1.0	11.6
+10 mM CFA + 1 mM IHP + 100 mM Cl^-	30	23 ± 2.0	9.3

Figure 5 shows some typical kinetic results obtained with dromedary hemoglobin under two extreme conditions (i.e., in the absence of allosteric factors and in the presence of all three cofactors), while Table IV reports the values for l at pH 6.5 obtained at 20 °C for all experimental conditions, i.e., the same as reported in Figures 1 and 2 for circular dichroism and in Figures 3 and 4 for XANES spectroscopy. It appears evident that the addition of either IHP (stoichiometric amount 1/1 with heme) or CFA (10 mM) brings about a slight but unequivocable enhancement of the overall CO dissociation rate constant, even though to a different extent for the two effectors (see Table IV). On the other hand, the presence of both anions together (IHP at a concentration 1 mM and CFA at 10 mM) induces a reversed behavior, canceling out the influence observed when they were present separately. This feature suggests a sort of negative contribution arising from the two interacting sites for the two effectors, such that their contemporary presence leads back to a functional (and possibly structural) situation comparable with that in the absence of both heterotropic ligands. Lastly, the addition of chloride ions (0.1 M) in the presence of both effectors brings about a marked enhancement of the CO dissociation rate constant, decreasing the activation free energy of the process by about 0.6 kcal·mol^{-1} (2.51 kJ·mol^{-1}) (see Figure 5 and Table IV).

Discussion

The system of dromedary hemoglobin is particularly suited to study the structural–functional interrelationships between heterotropic and homotropic sites (Amiconi et al., 1985; Santucci et al., 1986; Santucci & Amiconi, 1988). Thus the reported results indicate that intersubunit conformational changes of dromedary HbCO are very sensitive to the nature of the solvent, such that after addition of three anions (IHP, CFA, and chloride) a partial quaternary change toward the T state is observed. However, even without significantly affecting the overall stability of the R quaternary structure, the

addition of only one allosteric effector, such as IHP at a concentration equimolar with the tetrameric protein or CFA, brings about alterations of the tertiary local conformations, as detected by circular dichroism and XANES spectroscopy. Thus, the local structural changes around the irons in heme pockets of dromedary HbCO, induced by solvent components, may be summarized as follows: (i) the flattened porphyrins of dromedary HbCO in pure buffer become clearly domed only when a tertiary t conformation (as monitored by the appearance of a dichroic peak at 264 nm) is observed (see Table I and Figure 1); (ii) changes in the Fe–C–O bonding angle parallel porphyrin doming (see Tables I and II); (iii) two classes of Fe–C–O bonding angles appear to be stabilized in dromedary HbCO by solvent components [one is constituted by the protein in pure buffer, in IHP (equimolar with tetrameric protein), and in IHP (in molar excess) + CFA, with a Fe–C–O value more similar to that observed in human HbCO (i.e., 165°; see Bianconi et al., 1985c), and the other one (closer to 150°, i.e., to the value typical of MbCO; see Bianconi et al., 1985c) is induced by CFA or IHP (in molar excess) + CFA + Cl^-]; (iv) the distortion of the octahedral ligand field is not related in a simple way to other changes in the heme structural parameters.

In particular, addition of IHP in stoichiometric amount with respect to tetrameric dromedary HbCO shows no effect on the Fe–C–O bond angle (see Table I) and only a minor influence on the doming of the heme (to which the alteration of the shoulder at 264 nm of the dichroic spectra seems to be related). Conversely, the addition of CFA induces a marked tertiary conformation characterized by a significant change of the Fe–C–O bonding angle, of the Fe–N_ϵ distance, and of heme doming (see Tables I–III), all these events being accompanied by a variation of the dichroic spectra in the 264-nm region and by an enhancement of the CO dissociation rate constant.

However, when two organic anions (i.e., IHP and CFA) are present together in the system, the dichroic peak at 264 nm is lost and a shoulder appears, so that the dichroic spectrum as a whole assumes again a shape roughly reminiscent of that observed in the absence of allosteric effectors (i.e., that typical of high-affinity structure). In particular, the shape of the differential dichroic spectrum of the IHP + CFA system relative to the pure buffer is quite different from that (characterized by two peaks) induced by solvents that generate the dichroic feature at 264 nm (see Figure 2). Under the same solvent conditions, XANES features indicate only a change in the symmetry of the octahedral ligand field and a slight movement of the proximal histidine from the heme plane, though to a lesser extent than in the case of CFA (see Table III). On the other hand, no variation in the Fe–C–O bonding angle or in porphyrin doming is observed. In other words, the binding free energies to the protein of CFA and IHP propagate (by a mechanism that does not involve the dichroic absorbers) only to the irons, apparently without affecting the remainder of the heme; the resulting overall conformation of the subunits, therefore, is intermediate between Rr (as in the absence of effectors) and Rt (clearly observed when CFA alone is present). In this respect, it should be pointed out from all the reported observations that the trend in structural alteration occurring in dromedary HbCO tertiary conformation (as suggested mainly by the shoulder-peak transition at 264 nm in dichroic spectra) appears to be related mostly to XANES feature D (i.e., to the doming of the heme plane).

Finally, the addition of all three anions (IHP, CFA, and chloride) brings about in dromedary HbCO a partial switch of quaternary structure toward the T state (see Figures 1e and 2). However, if we compare such an effect, which amounts to about 45% of the protein in T structure (calculated from spectra typical of 100% R structure with 100% T structure; see Santucci & Amiconi, 1988), to the purely tertiary transition (Rr $\rightleftharpoons$ Rt) induced by CFA, we must notice that the quaternary switch is not accompanied by further peculiar changes in heme structural parameters, which (with the exception of the distortion of the octahedral field) are similar in magnitude (see Tables I–III) to those observed already in the presence of CFA alone. This evidence suggests that the ligated heme in dromedary hemoglobin is apparently flexible in its response to local environment, even in the absence of quaternary structural changes. In other words, the results indicate that there is not a unique, strong coupling between all stereochemical changes at the heme and quaternary structure, even though there should be some question as to whether dromedary HbCO ever adopts a true ligated T structure under the solvent conditions used; in fact, the characterization of quaternary conformational changes by dichroic spectra is confined only to one structural region which happens to be observable [i.e., Trp β 37(C3) and its environment].

Lastly, it is interesting to consider the above reported structural evidence (changes in dichroism and XANES spectroscopy) also in relation to the kinetic data. A good coupling between the primary bond process at the heme (e.g., CO dissociation rate) and structural observations is evident. Thus, there is a satisfactory correlation between the effector-induced variation of the CO dissociation rate constant and the dichroic peak at 264 nm as well as the heme doming; in fact, both the peak formation at 264 nm (Figure 1) and the increase of D/α_0 values (Table I) are accompanied by rate enhancement for CO dissociation (see Table IV). This observation is in line with the idea that the protein conformation not only is an active participant in the ligand binding mechanism but also provides most of the machinery by interconverting conformational free energy into electronic potential energy [the so-called rack mechanism (Lumry & Eyring, 1954; Lumry, 1961)], thus supporting the already suggested importance of electronic factors in determining the rate-limiting step of the CO dissociation process (Sharma et al., 1976).

In conclusion, the experiments reported above support what follows: (i) The ligated heme in dromedary hemoglobin is apparently very flexible in its response to the changing of tertiary environment by solvent components, even without quaternary changes. (ii) Although large variations in tertiary conformations may occur, essentially two classes of heme doming, Fe–C–O bonding angles, and ligand field distortion are observed; this is in agreement with the well-known, sharp spectral isosbestic points in oxygenation, indicating the existence of two and only two electronic states of the heme complex in spite of large variations in tertiary conformations. This might be a consequence of the weakness of the secondary interactions responsible for protein folding. (iii) The quaternary structure is not the unique dominant factor determining the tertiary environment around the heme; however, only quaternary conformational changes are able to affect at the same time all stereochemical modifications at the heme (including distortion of the ligand field).

Registry No. Heme, 14875-96-8; IHP, 83-86-3; CFA, 882-09-7; Fe, 7439-86-3; O, 7782-44-7; Cl, 16887-00-6.

References

Abraham, D. J., Perutz, M. F., & Phillips, S. E. V. (1983) *Proc. Natl. Acad. Sci. U.S.A. 80*, 324–328.

Ackers, G. K., & Smith, F. R. (1987) *Annu. Rev. Biophys. Chem. 16*, 583–609.

Amiconi, G., & Giardina, B. (1981) *Methods Enzymol. 76*, 533–552.

Amiconi, G., Bertollini, A., Bellelli, A., Coletta, M., Condò, S. G., & Brunori, M. (1985) *Eur. J. Biochem. 150*, 387–393.

Antonini, E., & Gibson, Q. H. (1960) *Biochem. J. 76*, 534–538.

Antonini, E., & Brunori, M. (1971) *Hemoglobin and Myoglobin in their Reactions with Ligands*, North-Holland, London.

Arnone, A., Rogers, P., Blough, N. V., McGourty, J. L., & Hoffman, B. M. (1976) *J. Mol. Biol. 188*, 693–706.

Baldwin, J., & Chothia, C. (1979) *J. Mol. Biol. 129*, 175–220.

Bertollini, A., Santucci, R., Amiconi, G., Ascoli, F., Currell, D. L., Mursal, O., & Brunori, M. (1988) *Eur. J. Biochem. 176*, 669–673.

Bianconi, A. (1987) in *X-Ray Absorption: Principle, Applications, Techniques: EXAFS, SEXAFS and XANES* (Prinz, R., & Konigsberger, D. C., Eds.) pp 167–174, Wiley, New York.

Bianconi, A., Congiu Castellano, A., Dell'Ariccia, M., Giovannelli, A., Burattini, E., Castagnola, M. E., & Durham, P. J. (1985a) *Biochim. Biophys. Acta 831*, 120–124.

Bianconi, A., Congiu Castellano, A., Dell'Ariccia, M., Giovannelli, A., Burattini, E., Durham, P. J., Giacometti, G. M., & Morante, S. (1985b) *Biochim. Biophys. Acta 831*, 114–119.

Bianconi, A., Congiu Castellano, A., Durham, P. J., Hasnain, S. S., & Phillips, S. (1985c) *Nature 318*, 685–687.

Bianconi, A., Congiu Castellano, A., Dell'Ariccia, M., Giovannelli, A., Burattini, E., & Durham, P. J. (1985d) *Biochem. Biophys. Res. Commun. 131*, 98–102.

Braunitzer, G., Schrank, B., Stangl, A., & Wiesner, H. (1979) *Hoppe-Seyler's Z. Physiol. Chem. 360*, 1941–1944.

Brunori, M., Coletta, M., & Giardina, B. (1985) *Metalloproteins* (Harrison, P., Ed.) Vol. II, pp 263–331, Macmillan, London.

Cartier, C., Momenteau, M., Dartyge, E., Fontaine, A., Tourillon, G., Bianconi, A., & Verdaguer, M. (1988) *J. Am. Chem. Soc.* (submitted for publication).

Desideri, A., Ascenzi, P., Chiancone, E., & Amiconi, G. (1987) *J. Inorg. Biochem. 29*, 131–135.

Edelstein, S. G. (1975) *Annu. Rev. Biochem. 44*, 209–232.

Gelin, B. R., Lee, A. W.-M., & Karplus, M. (1983) *J. Mol. Biol. 171*, 489–559.

Geraci, G., & Parkhust, L. J. (1981) *Methods Enzymol. 76*, 262–274.

Lumry, R. (1961) *Biophysics (Toyonaka, Jpn.) 1*, 109–114.

Lumry, R., & Eyring, H. (1954) *J. Phys. Chem. 58*, 110–120.

Morante, S., Congiu Castellano, A., Dell'Ariccia, M., Durham, P. J., Giovannelli, A., Burattini, E., & Bianconi, A. (1987) in *Biophysics and Synchrotron Radiation* (Bianconi, A., & Congiu Castellano, A., Eds.) pp 107–113, Springer Verlag, New York.

Oyanagi, H., Iizuka, T., Matsushita, T., Saigo, S., Makino, R., & Ishimura, Y. (1987) in *Biophysics and Synchrotron Radiation* (Bianconi, A., & Congiu Castellano, A., Eds.) pp 100–106, Springer Verlag, New York.

Perutz, M. F. (1972) *Nature 237*, 495–499.

Perutz, M. F. (1979) *Annu. Rev. Biochem. 48*, 327–386.

Perutz, M. F., & Poyart, C. (1983) *Lancet 2*, 881–882.

Perutz, M. F., Fersht, M. R., Simon, F. R., & Roberts, G. C. K. (1974) *Biochemistry 13*, 2174–2186.

Perutz, M. F., Fermi, G., Luisi, B., Shaanan, B., & Liddington, R. C. (1987) *Acc. Chem. Res. 20*, 309–321.

Rousseau, D. L., & Ondrias, M. R. (1983) *Annu. Rev. Biophys. Bioeng. 12*, 357–380.

Santucci, R., & Amiconi, G. (1988) *Biol. Chem. Hoppe-Seyler 369*, 251–256.

Santucci, R., Ascoli, F., Bertollini, A., Amiconi, G., & Brunori, M. (1985) *Biochem. J. 231*, 793–796.

Santucci, R., Ascoli, F., Amiconi, G., & Brunori, M. (1986a) *Biochem. J. 235*, 791–795.

Santucci, R., Amiconi, G., Ascoli, F., & Brunori, M. (1986b) *Biochem. J. 240*, 613–616.

Sharma, V. S., Ranney, H. M., Geibel, J. F., & Traylor, T. G. (1975) *Biochem. Biophys. Res. Commun. 66*, 1301–1306.

Sharma, V. S., Schmidt, M. R., & Ranney, H. M. (1976) *J. Biol. Chem. 251*, 4267–4272.

Warshel, A. (1977) *Proc. Natl. Acad. Sci. U.S.A. 74*, 1789–1793.